

ARTICLE

Kinetic-Pharmacodynamic Model of Platelet Time Course in Patients With Moderate-to-Severe Atopic Dermatitis Treated With Oral Janus Kinase 1 Inhibitor Abrocitinib

Elena Soto¹, Christopher Banfield², Pankaj Gupta² and Mark C. Peterson^{2*}

The oral Janus kinase 1 (JAK1) inhibitor abrocitinib reduced signs and symptoms of atopic dermatitis (AD) in a placebo-controlled, randomized, double-blind, phase IIb trial (dose range 10–200 mg). A kinetic-pharmacodynamic (K-PD) model consisting of proliferation, maturation, and blood circulation compartments was developed to characterize platelet count changes during the study. The K-PD model consisted of a drug elimination constant, four system parameters describing platelet dynamics, variance terms, correlation, and residual errors. Overall, these patients exhibited mean transit time from progenitor cells to platelets of 8.2 days (longer than the reported megakaryocyte life span), likely arising from JAK1-induced perturbations of platelet progenitor homeostasis. The final model described dose-related platelet count declines until nadir at treatment week 4 and return to baseline levels thereafter. The model was deemed suitable to support the design of subsequent abrocitinib AD trials and indicated limited clinically relevant platelet reductions in the range of doses studied.

Study Highlights

WHAT IS THE CURRENT KNOWLEDGE ON THE TOPIC?

✓ Descriptions in the literature of the dose-response relationship between selective Janus kinase 1 (JAK1) inhibition and hematology outcomes are limited.

WHAT QUESTION DID THIS STUDY ADDRESS?

✓ The current analysis addressed whether a parametric model could be developed to describe the relationship between JAK1 inhibitor administered dose and platelet count over time.

WHAT DOES THIS STUDY ADD TO OUR KNOWLEDGE?

✓ The results demonstrate that JAK1 inhibitor dose can be linked to changes in platelet counts over time and suggest the impact of a range of doses that can be evaluated in subsequent clinical trials.

HOW MIGHT THIS CHANGE DRUG DISCOVERY, DEVELOPMENT, AND/OR THERAPEUTICS?

✓ The semimechanistic model developed here may be suitable for simulation purposes to support further trial designs for abrocitinib and/or other JAK inhibitors.

Atopic dermatitis (AD) is a common, chronic, relapsing inflammatory skin disease that poses a significant disease burden and affects patient quality of life.¹ Although AD prevalence varies by region, it affects up to 20% of children and 3% of adults worldwide.¹ Abrocitinib (previously PF-04965842) is an oral Janus kinase 1 (JAK1) selective inhibitor under investigation for the treatment of AD.

AD is characterized by the activation of several cytokine signaling pathways involving type 1 helper T-cells (Th1), Th2, Th22, and Th17 lymphocytes, suggesting that dysregulation of immune responses leads to the diverse manifestations of the disease.² JAKs—JAK1, JAK2, JAK3, and tyrosine kinase 2 (TYK2)—are a family of nonreceptor tyrosine kinases that play a key role in signaling events in innate and adaptive immunity and the maturation of hematopoietic cells.³ Positive results have been reported for oral JAK inhibitors, including abrocitinib in AD trials.^{4–8} In a phase IIb study, 200-mg and

100-mg once-daily doses of abrocitinib resulted in significantly higher Investigator's Global Assessment response rates than placebo at week 12 (primary end point) in adults with moderate-to-severe AD, with mostly mild adverse events that were considered unrelated to treatment.⁵ Dose-related changes in platelet counts were observed for all doses \geq 10 mg.⁵ Anemia and thrombocytopenia are thought to be “on-target” effects of JAK inhibitors. These are usually dose-dependent and influenced by baseline platelet count, as observed in phase I/II trials in other indications.⁹

Semimechanistic pharmacokinetic-pharmacodynamic (PK-PD) and kinetic (K)-PD models have been used previously to characterize drug effects on platelet counts in other indications.^{10–12} In the absence of PK data, K-PD modeling has been shown to be a viable approach and provides parameter estimates that are in good agreement with those obtained through PK-PD analysis.¹³ K-PD modeling

¹Pfizer UK Limited, Sandwich, UK; ²Pfizer Inc., Cambridge, Massachusetts, USA. *Correspondence: Mark C. Peterson (Mark_Peterson@vrtx.com)
Received: September 25, 2019; accepted: June 30, 2020. doi:10.1002/psp4.12548

has been successfully applied to various drugs and drug effects^{14–16}; it performed well in the analysis of data involving a wide range of doses and dose intervals and has been demonstrated to be useful in simulations. However, it should be noted that K-PD model performance deteriorates in terms of bias, precision, and convergence when interindividual and residual variabilities are high.¹³

To characterize the dose-response relationship of abrocitinib with platelet count fluctuations observed in the phase IIb study of patients with AD, we applied a semimechanistic K-PD model and used it to simulate platelet counts following a range of abrocitinib doses.

METHODS

Study design and procedures

The design of the multicenter, randomized, double-blind phase IIb dose-ranging study has been described previously.⁵ Briefly, adults with moderate-to-severe AD (percentage of affected body surface area ≥ 10 , Eczema Area and Severity Index ≥ 12 , and Investigator's Global Assessment ≥ 3) for ≥ 1 year and documented history of inadequate response to topical treatment (given ≥ 4 weeks), or for whom topical treatments were otherwise medically inadvisable, were randomly assigned 1:1:1:1 to once-daily oral abrocitinib (200, 100, 30, or 10 mg) or placebo for 12 weeks, followed by a 4-week treatment-free follow-up period. Platelet counts were measured at screening; baseline; weeks 1, 2, 4, 6, 8, and 12 (on treatment); and weeks 13, 14, and 16 (off-treatment follow-up).

Model development

The model was developed and fitted to the trial data using a two-stage process, wherein initially placebo data were excluded followed by the inclusion of placebo data. Model fitting was performed using nonlinear mixed-effects maximum likelihood methods (NONMEM; version 7.3; ICON Development Solutions, Hanover, MD), supported with Perl-speaks-NONMEM (version 4.2.0; Uppsala University, Uppsala, Sweden). Exploratory data analysis and creation of graphs were conducted in R (version 3.0.2 or above) implemented within R-Studio.

K-PD model

Because no abrocitinib concentration data were available at the time of modeling, a dose-response K-PD model was developed. The link from abrocitinib dose to drug effect was described using a virtual one-compartment model with bolus input. The elimination constant k_e , multiplied by DrugAmount, corresponds to the elimination rate from that virtual compartment as follows:

$$\frac{d_{\text{DrugAmount}}}{dt} = -k_e \cdot \text{DrugAmount}$$

The resulting drug effect, assumed to affect platelet precursor production, was described by a linear model consisting of DrugAmount at a given time multiplied by a Slope parameter as follows:

$$\text{Drug effect} = \text{DrugAmount} \cdot \text{Slope}$$

PD semimechanistic model

The semimechanistic model was based on the PK-PD myelosuppression model developed by Friberg *et al.*,¹⁷ which has previously been used to describe the time course of leukocyte, neutrophil, and platelet counts.^{10,12,18} The model consisted of a platelet proliferation pool (Prol) representing platelet progenitor cells, transit compartments (T_1 , T_2 , and T_3) to mimic the maturation of megakaryoblasts and megakaryocytes into platelets, and a compartment representing circulating platelets (**Figure 1**). The maturation chain with compartments and rate constants (k_{tr}) allowed the description of the time delay from the start of treatment, maximum effect, and subsequent re-equilibration to steady-state. In the model, the generation of platelets depended on the number of cells in the Prol compartment, the synthesis rate constant (k_{syn}), the feedback effect from circulating platelets (Rbd), and the drug effect. Platelets were eliminated from circulation at a first-order rate described by the product of an elimination rate constant (k_{el}) and circulating platelet count (CircP), with k_{el} assumed to be the same as k_{tr} to simplify the model. The PD model is described by the following differential equations:

$$\frac{d_{\text{Prol}}}{dt} = k_{syn} \cdot \text{Prol} \cdot \text{Rbd} \cdot (1 - \text{Drug effect}) - k_{tr} \cdot \text{Prol}$$

$$\frac{d_{T1}}{dt} = k_{tr} \cdot \text{Prol} - k_{tr} \cdot T_1$$

$$\frac{d_{T2}}{dt} = k_{tr} \cdot T_1 - k_{tr} \cdot T_2$$

$$\frac{d_{T3}}{dt} = k_{tr} \cdot T_2 - k_{tr} \cdot T_3$$

$$\frac{d_{\text{CircP}}}{dt} = k_{tr} \cdot T_3 - k_{el} \cdot \text{CircP}$$

where Rbd consisted of circulating platelet count at baseline (CircP_0) divided by circulating platelet count at time t (CircP) raised to the power of the feedback parameter, γ , as follows:

$$\text{Rbd} = \left(\frac{\text{CircP}_0}{\text{CircP}} \right)^\gamma$$

Random effects model

Interindividual variability (IIV) was modeled using multiplicative exponential random effects taking the following form:

$$\theta_i = \theta \cdot \exp^{\eta_i}$$

where θ is the population typical value of the parameter, θ_i is the individual value of the parameter, and η_i is the inter-individual random effect accounting for the i^{th} individual's deviation from the typical value θ . The distribution of η_i values in the population is assumed to be normally distributed, with a mean of zero and variance ω^2 . The approximate

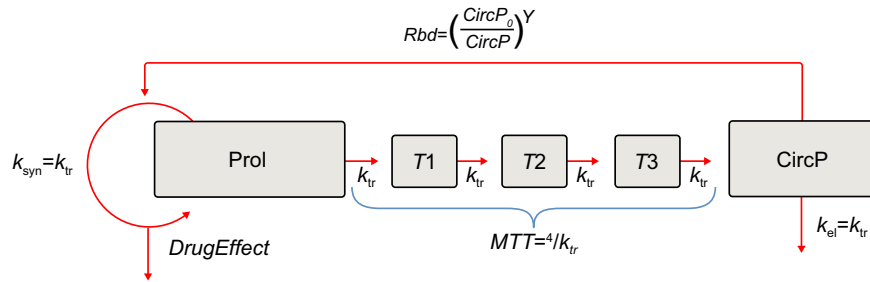


Figure 1 Platelet synthesis semimechanistic model scheme. γ , feedback parameter; CircP, circulating platelets at time t ; CircP₀, circulating platelets at baseline; k_{el} , elimination rate constant; k_{syn} , synthesis rate constant; k_{tr} , transit rate constant; MTT, mean transit time; Prol, platelet proliferation pool; Rbd, feedback effect from circulating platelets; T , maturation compartments.

percentage coefficient of variation (%CV) within the study population was calculated as:

$$\%CV = \sqrt{\omega^2} \cdot 100.$$

Residual variability was modeled with a combination, additive plus proportional error structure as follows:

$$Y_{ij} = F_{ij} + \epsilon 1_{ij} + F_{ij} \cdot \epsilon 2_{ij}$$

where Y_{ij} is the observed platelet count for the i^{th} individual at the j^{th} time point, F_{ij} is the predicted platelet count, and $\epsilon 1_{ij}$ and $\epsilon 2_{ij}$ are the additive and proportional errors, respectively, for the i^{th} individual at the j^{th} time point. As with the IIV, the population distributions of the residual error terms were assumed to be normally distributed, having means of zero and variance estimates σ_1^2 and σ_2^2 , respectively.

Model assessment

Final model evaluation was completed by conducting visual predictive checks with 1,000 simulations summarized as the 5th, 50th, and 95th quantiles of the predicted platelets counts and the 5th and 95th quantiles/uncertainties of each of those three metrics.

Simulations

Simulations were performed using the final model and estimated parameters, with datasets that consisted of 300 virtual subjects receiving abrocitinib once daily for 12 weeks and having seven simulated sample times that correspond to the actual sample times collected during the study (at weeks 0, 1, 2, 4, 6, 8, and 12). To visualize the dose-response profile, doses ranging from 0–200 mg at 25-mg increments were simulated 1,000 times at each dose level.

From the simulated data, the proportion of patients with platelet counts within each clinical grade were summarized. In addition, incremental changes in platelet levels within grade 1 were evaluated to further assess whether doses produced near-normal platelet levels. Therefore, the thrombocytopenia levels shown in this work do not exactly match clinical grades of thrombocytopenia. These levels (summarized as median and 5th and 95th percentiles) are the platelet counts under 50,000/ μL (thrombocytopenia grade ≥ 3), under 75,000/ μL (thrombocytopenia grade ≥ 2), under 100,000/ μL (thrombocytopenia grade ≥ 2 and a portion of

grade 1 levels), 125,000/ μL (thrombocytopenia grade ≥ 2 and a portion of grade 1 levels), and 150,000/ μL (thrombocytopenia grade ≥ 1).

RESULTS

Data for analysis

A total of 267 patients received at least 1 dose of study treatment (200 mg, $n = 55$; 100 mg, $n = 56$; 30 mg, $n = 51$; 10 mg, $n = 49$; and placebo, $n = 56$). Of these, five patients were not included in this analysis because of questionable and unreconcilable date/time records ($n = 3$), NONMEM numeric difficulties ($n = 1$), and absence of platelet counts ($n = 1$). Two patients who were randomized but did not receive study treatment were added to the remaining 262 patients, contributing screening and baseline platelet counts. Therefore, 2,330 platelet counts from a total of 264 patients were used in the analysis.

Platelet baseline levels were similar between treatment groups and ranged from 268,000–284,000/ μL . The platelet counts from baseline and over the duration of study for each treatment group are shown in **Figure 2a** with mean percentage change in platelet counts from baseline through time for each treatment group in **Figure 2b**. From treatment initiation to week 4, the median decline in platelet counts were 11% and 29% in the 100-mg and 200-mg abrocitinib groups, respectively. Following the nadir, platelet counts in both dose groups returned toward baseline levels, establishing median steady-state levels of 8% and 15% below baseline by week 12 (end of treatment) in the 100-mg and 200-mg abrocitinib groups, respectively. With extended follow-up to week 16, platelet counts increased toward baseline values in all dose groups, with a mild elevation in the 100-mg and 200-mg dose groups.

Model results

Model parameters were estimated with adequate precision (**Table 1**), except for the correlation between IIVs, which had a high relative standard error believed to arise primarily from the very small correlation (-0.0258). A linear model was adequate to describe the drug effect; improvement in the fit was not significant with a maximum effect (E_{max}) model that was also tested (assessed by the decrease in the objective function value; data not shown). The final model described the small changes in platelet count observed for the 30-mg treatment group throughout treatment as well as the larger, dose-dependent decreases in

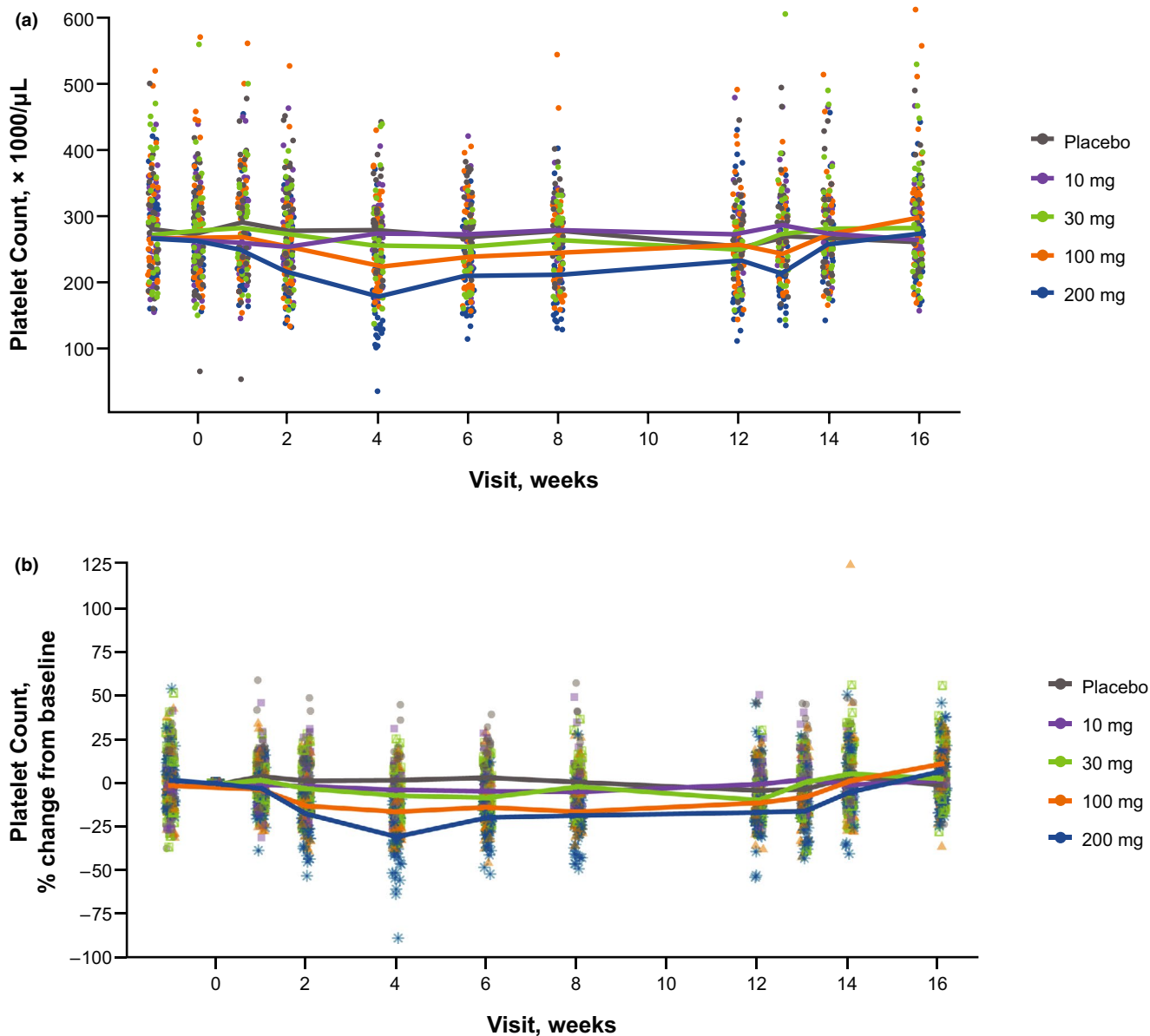


Figure 2 Platelet count time course for each treatment group. Platelet count (a) and percentage change from baseline in platelet count (b). Lines correspond to median per treatment group.

Table 1 Parameters estimates for the final model

Parameter, units	Estimate	RSE, %
k_e , hour ⁻¹	0.278	NA
BASE, × 1,000/μL	272	1.32
MTT, hour	197	5.7
Slope, mg ⁻¹	0.00231	10.8
γ	0.314	10.6
Residual error (additive), × 1,000/μL	13.6	41.2
Residual error (proportional), %	9.83	12.8
IIV on BASE, %	21.2	13.9
IIV on slope, %	60	20.7
Correlation	-0.0258	444

γ , feedback parameter; BASE, platelet baseline levels; IIV, interindividual variability; k_e , elimination rate constant; MTT, mean transit time; NA, not applicable; RSE, relative standard error.

platelet count (until week 4), followed by increases toward baseline levels for the 100-mg and 200-mg abrocitinib groups (**Figure 3**).

Simulations

Using the final model, the projected incidence rates for each minimum platelet count threshold, associated with different grades of thrombocytopenia, were generated for doses 0–200 mg at 25-mg increments. The dose levels corresponding to those of the trial were compared with observed data. Thrombocytopenia level grade ≥ 1 (“below 150,000/μL” and “below 125,000/μL”) platelet count threshold groups were better predicted, particularly at higher abrocitinib doses (**Figure 4**). The projected incidence rates for these two threshold groups at lower doses appeared to be overpredicted, potentially due to a small number of low platelet counts observed.

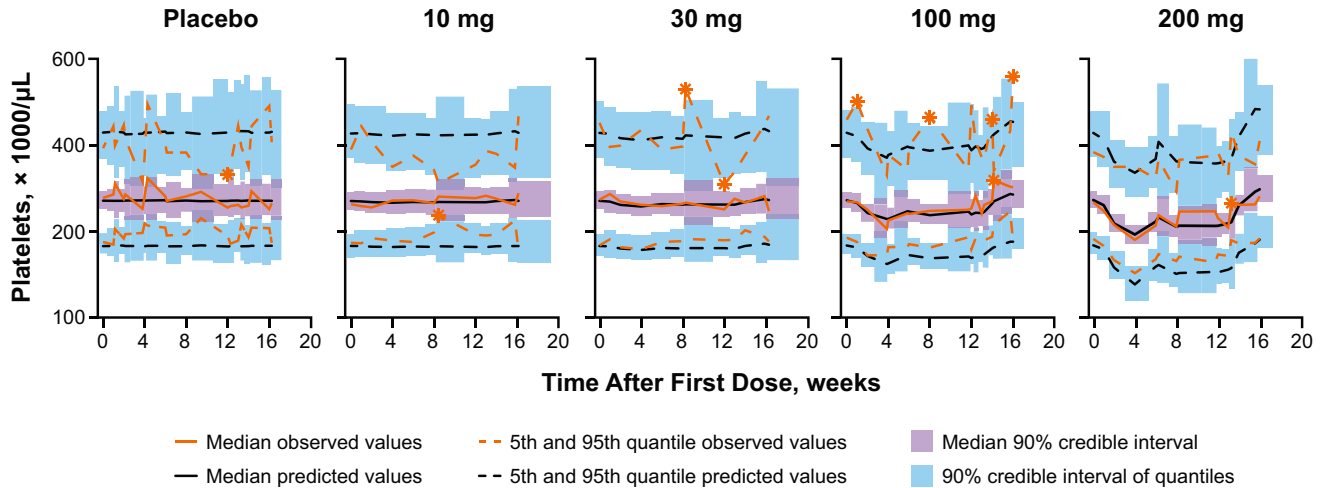


Figure 3 Final model visual predictive check.

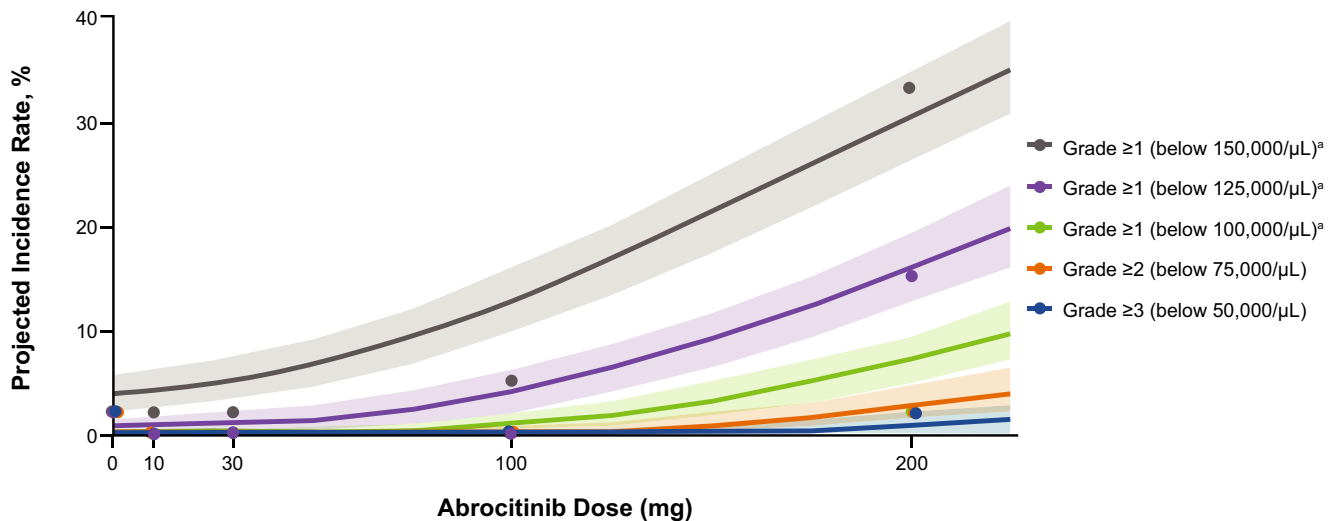


Figure 4 Projected incidence rates for threshold platelet counts for abrocitinib and observed incidence rates for abrocitinib doses at individual nadirs. Abrocitinib doses ranged from 0 to 200 mg, in 25-mg increments. Shaded areas are projected incidence rates; data points are observed incidence rates. ^aGrade 1 includes platelets levels between 75,000–150,000/μL. For this simulation, grade 1 levels were further divided in a grade 1 level < 125,000/μL and < 100,000/μL.

Because the nadir in platelet count was observed at approximately week 4, two additional time-dependent metrics were derived from the simulations—an assessment of the thresholds during the initial treatment period (weeks 0, 1, 2, or 4; **Figure 5a**) and for the later treatment period (weeks 6, 8, or 12; **Figure 5b**). These metrics showed that platelet counts decrease mostly in the initial treatment period, with lower incidence of platelet count decrease in the later treatment period.

DISCUSSION

During the rapid course of drug development, modeling- and simulation-informed go/no-go decisions are often based on available data instead of delaying until additional data become available. Although this time pressure is understandable on the broader scale of drug

development timelines, it has consequences for the methods chosen for analyses supporting advancement decisions. In this context, quantification of the effects of abrocitinib on platelet count during treatment and after treatment discontinuation was sought in advance of the availability of abrocitinib population PK data. Therefore, a K-PD modeling approach was applied to expeditiously inform understanding of this relationship. A semimechanistic model consisting of a progenitor pool, three maturation compartments, a circulation compartment, and negative feedback effect generated by circulating platelets relative to baseline was utilized to describe and quantify the observed platelet count data from a phase IIb proof-of-concept trial of abrocitinib in patients with moderate-to-severe AD. This approach described platelet changes arising from inhibition of platelet production as a function of abrocitinib dose in a manner consistent with

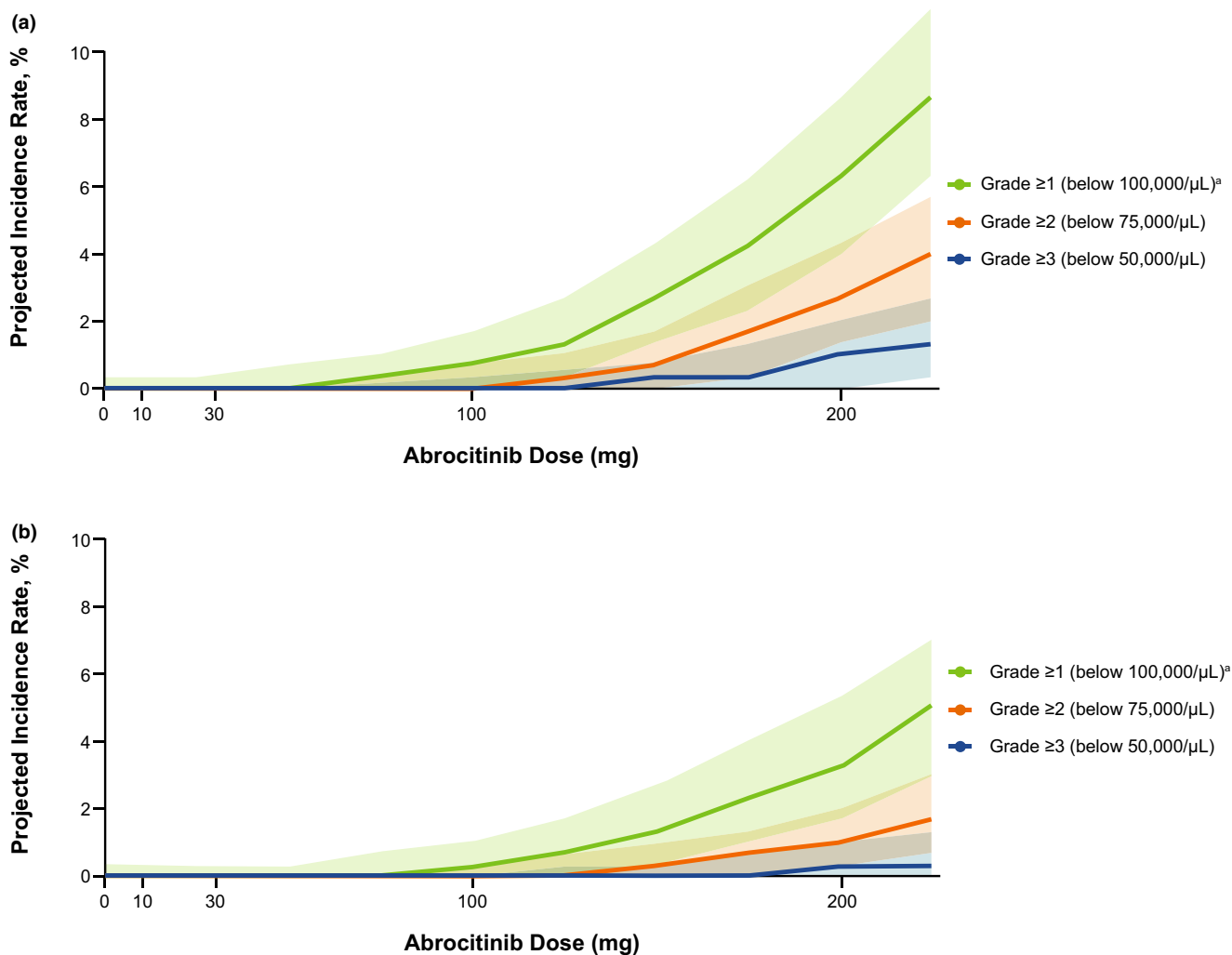


Figure 5 Projected incidence rates for threshold platelets counts at nadir for abrocitinib. During the first 4 weeks of treatment (a), and during the last 6 weeks of treatment (b). Abrocitinib doses ranged from 0 to 200 mg, in 25 mg increments. Shaded areas are projected incidence rates. ^aIncludes grade 1 levels below 100,000/ μL only, plus grades 2, 3, and 4.

previously published models.^{10–12} Although it is known that JAK2, thrombopoietin, interleukin 6, and other cytokines are involved in platelet homeostasis, the goal of the current K-PD model development was to characterize the dynamic nature of the observed data with limited information using a heuristic, stochastic model suitable for subsequent informative simulations in a short timeframe.

The relationship between platelet count and JAK-related physiologic mechanisms has been described recently using a systems pharmacology model that incorporated several mechanisms of platelet regulation.¹⁹ The model proposed that megakaryoblast production is attenuated and megakaryocyte expansion is allowed through the indirect actions of JAK inhibition. This results in a slower than normal maturation of megakaryoblasts and megakaryocytes to platelets, and a larger than normal progenitor pool. In our K-PD model, the mean transit time (MTT) was estimated to be 8.2 days, similar to MTT values described previously^{11,12} but longer than the reported megakaryocyte life span.²⁰

In this K-PD model, the rate of platelet elimination was the same as the rate of precursor cells moving through the maturation compartments. Therefore, the estimation of longer MTT is related to smaller values of k_{tr} and k_{el} .²¹ Although this may not reflect the physiology of platelets in individuals without AD exactly, this approximation describes the observed data well, and provides insights into the delicate homeostatic mechanisms that control platelet count. In addition, whereas the physiology of platelet maturation and elimination is complex, involving feedback loops and cytokines, the presented model represents a fit-for-purpose model that provided answers to important questions relevant for subsequent abrocitinib trial designs, such as time to platelet count nadir and extent of platelet count reduction.

Overall, the model performed well in its ability to describe the observed platelet count data over the investigated dose range. For abrocitinib doses ≤ 30 mg, the model recapitulated the observed dose-dependent changes in platelets, with model-generated variability across and within patients that was consistent with the trial results. For the 100-mg

and 200-mg abrocitinib doses, the model was able to characterize the larger, dose-dependent decline in platelet counts until the nadir at ~ 4 weeks after treatment initiation, as well as the post-nadir levels, and the return to baseline levels. The projected percentage incidence rates of platelet count below 150,000/ μ L and 125,000/ μ L were in reasonable agreement with the observed data, especially at higher doses. The minimal effect of abrocitinib on platelet count at low doses resulted in few events observed below the count thresholds of < 150,000/ μ L and < 100,000/ μ L. This result, compounded by the size limitations of the cohorts investigated, means that the simulations populated the details of the distribution more fully than the observed data, thus differing in these distribution regions (i.e., thresholds < 150,000/ μ L and < 100,000/ μ L). As it is reasonable to expect larger sample sizes to be needed to adequately characterize the extremes of distributions, the differing outcome from these larger simulations compared with the substantially smaller trial sample is not unexpected. Nonetheless, the platelet count effect of abrocitinib 30 mg is small, and the simulated outcomes are consistent with this observation.

An important element of this modeling and simulation was the insights provided into both the time-dependent and dose-response effects of abrocitinib to aid in designing a subsequent trial. As the dynamics of platelets are variable, the maturation compartments included in the model provided a platform to explore what is expected as a function of time as the levels decrease and then establish a revised steady state. The overall predicted platelet levels can be dissected into two distinct periods: that before reaching the platelet nadir and that beyond that time to end of treatment at 12 weeks. The model suggests that the possibility for higher-grade thrombocytopenia decreases nearly 50% after the first 4 weeks of abrocitinib treatment and remains at that reduced level until the end of treatment. The dose response predicts that at 100-mg and 200-mg doses there is a mean (90% prediction interval) of 0% (0.0–0.7%) and 2.7% (1.3–4.3%) expected incidence rate of grade ≥ 2 thrombocytopenia ($\leq 75,000$ platelets/ μ L), respectively, over a 12-week period of treatment. Although further clinical investigation will bolster the available data and improve the understanding of platelet homeostasis during abrocitinib treatment, the current modeling and simulations can support subsequent clinical trial design decisions regarding dose and treatment duration.

There are limitations to the model developed in this study. First, the model depends on observation intervals and information content for parameter estimation. Thus, the chosen sampling times, length of dosing, and time of follow-up likely influenced parameter estimation, and, therefore, the predictive limits and capabilities of the model. This should be considered when viewing the simulated profiles arising from various doses. Second, this was a dose-response analysis rather than an exposure-response analysis, limiting the ability to further refine the effect of different drug exposures on platelet count and evaluating explicative covariates of interest. Future consideration of PK variability will aid in understanding the impact of this limitation in the current modeling. In addition, once concentrations become

available, covariates can be explored to facilitate better understanding of intersubject variability. However, the current K-PD model addresses that need for selection of doses in subsequent trials directly. Finally, the model used baseline assumptions for simulations that may not apply to different populations with respect to mechanism and initial platelet counts. Future use of the model should consider that effect on any simulated outcomes. With these considerations in mind, the degree to which platelet changes are manifested in a broader population and the clinical relevance will be assessed in subsequent clinical trials designed with the support of the current model.

CONCLUSIONS

For the oral JAK1 selective inhibitor abrocitinib, a K-PD model approach was adequate to quantify and predict the relationship between drug dose and its effect on platelet counts. This model can be used to understand the time- and dose-dependent effects of abrocitinib therapy on platelet count, thereby informing dose selections and designs for future studies of abrocitinib.

Acknowledgments. Editorial/medical writing support under the guidance of the authors was provided by Juan Sanchez-Cortes, PhD, at ApotheCom, San Francisco, CA, and was funded by Pfizer Inc., New York, NY, in accordance with Good Publication Practice (GPP3) guidelines (Ann. Intern. Med. 163, 461–464 (2015)). This study was sponsored by Pfizer, Inc.

Author Contributions. All authors wrote the manuscript. All authors designed and performed the research. E.S. analyzed the data.

Data Sharing. Upon request, and subject to certain criteria, conditions and exceptions (see <https://www.pfizer.com/science/clinical-trials/trial-data-and-results> for more information), Pfizer will provide access to individual de-identified participant data from Pfizer-sponsored global interventional clinical studies conducted for medicines, vaccines, and medical devices (1) for indications that have been approved in the United States and/or the European Union or (2) in programs that have been terminated (i.e., development for all indications has been discontinued). Pfizer will also consider requests for the protocol, data dictionary, and statistical analysis plan. Data may be requested from Pfizer trials 24 months after study completion. The de-identified participant data will be made available to researchers whose proposals meet the research criteria and other conditions, and for which an exception does not apply, via a secure portal. To gain access, data requestors must enter into a data access agreement with Pfizer.

1. Nutten, S. Atopic dermatitis: global epidemiology and risk factors. *Ann. Nutr. Metab.* **66** (suppl. 1), 8–16 (2015).
2. Brunner, P.M. et al. Early-onset pediatric atopic dermatitis is characterized by TH2/TH17/TH22-centered inflammation and lipid alterations. *J. Allergy Clin. Immunol.* **141**, 2094–2106 (2018).
3. Ghoreschi, K., Laurence, A. & O'Shea, J.J. Janus kinases in immune cell signaling. *Immunol. Rev.* **228**, 273–287 (2009).
4. Bissonnette, R. et al. Topical tofacitinib for atopic dermatitis: a phase IIa randomized trial. *Br. J. Dermatol.* **175**, 902–911 (2016).
5. Gooderham, M. et al. Efficacy and safety of oral Janus kinase 1 inhibitor abrocitinib for patients with atopic dermatitis. *JAMA Dermatol.* **155**, 1371 (2019).
6. Guttman-Yassky, E. et al. Baricitinib in adult patients with moderate-to-severe atopic dermatitis: a phase 2 parallel, double-blinded, randomized placebo-controlled multiple-dose study. *J. Am. Acad. Dermatol.* **80**, 913–921 (2019).
7. Guttman-Yassky, E. et al. Primary results from a phase 2b, randomized, placebo-controlled trial of upadacitinib for patients with atopic dermatitis. Presented at:

- 76th American Academy of Dermatology Annual Meeting; February 16–20, 2018; San Diego, CA. Abstract 6533.
8. Nakagawa, H., Nemoto, O., Igarashi, A. & Nagata, T. Efficacy and safety of topical JTE-052, a Janus kinase inhibitor, in Japanese adult patients with moderate-to-severe atopic dermatitis: a phase II, multicentre, randomized, vehicle-controlled clinical study. *Br. J. Dermatol.* **178**, 424–432 (2018).
 9. Gotlib, J. JAK inhibition in the myeloproliferative neoplasms: lessons learned from the bench and bedside. *Hematology Am. Soc. Hematol. Educ. Program* **2013**, 529–537 (2013).
 10. Bender, B.C. et al. A population pharmacokinetic/pharmacodynamic model of thrombocytopenia characterizing the effect of trastuzumab emtansine (T-DM1) on platelet counts in patients with HER2-positive metastatic breast cancer. *Cancer Chemother. Pharmacol.* **70**, 591–601 (2012).
 11. Perez-Ruixo, J.J., Green, B., Doshi, S., Wang, Y.M. & Mould, D.R. Romiplostim dose response in patients with immune thrombocytopenia. *J. Clin. Pharmacol.* **52**, 1540–1551 (2012).
 12. van Kesteren, C. et al. Semi-physiological model describing the hematological toxicity of the anti-cancer agent indisulam. *Invest. New Drugs* **23**, 225–234 (2005).
 13. Jacqmin, P. et al. Modelling response time profiles in the absence of drug concentrations: definition and performance evaluation of the K-PD model. *J. Pharmacokin. Pharmacodyn.* **34**, 57–85 (2007).
 14. Goggin, T. et al. Population PD(-PK) modeling and clinical trial simulation, characterizing schedule dependence of hematotoxicity and other phase II trial design features for a new oral anticancer drug. Presented at: 10th Annual Meeting of the Population Approach Group in Europe; June 7–8, 2001; Basel, Switzerland. Abstract 180 <<https://www.page-meeting.org/default.asp?abstract=180>>.
 15. Pan, S. et al. Pharmacodynamics of rituximab on B lymphocytes in paediatric patients with autoimmune diseases. *Br. J. Clin. Pharmacol.* **85**, 1790–1797 (2019).
 16. Romberg, R., Olofson, E., Sarton, E., Teppema, L. & Dahan, A. Pharmacodynamic effect of morphine-6-glucuronide versus morphine on hypoxic and hypercapnic breathing in healthy volunteers. *Anesthesiology* **99**, 788–798 (2003).
 17. Friberg, L.E., Henningson, A., Maas, H., Nguyen, L. & Karlsson, M.O. Model of chemotherapy-induced myelosuppression with parameter consistency across drugs. *J. Clin. Oncol.* **20**, 4713–4721 (2002).
 18. Tsuji, Y. et al. Population pharmacokinetics and pharmacodynamics of linezolid-induced thrombocytopenia in hospitalized patients. *Br. J. Clin. Pharmacol.* **83**, 1758–1772 (2017).
 19. Koride, S., Nayak, S., Banfield, C. & Peterson, M.C. Evaluating the role of Janus kinase pathways in platelet homeostasis using a systems modeling approach. *CPT Pharmacometrics Syst. Pharmacol.* **8**, 478–488 (2019).
 20. Machlus, K.R. & Italiano, J.E. Jr. The incredible journey: from megakaryocyte development to platelet formation. *J. Cell Biol.* **201**, 785–796 (2013).
 21. Najean, Y., Ardaillou, N. & Dresch, C. Platelet lifespan. *Annu. Rev. Med.* **20**, 47–62 (1969).

© 2020 Pfizer Inc. *CPT: Pharmacometrics & Systems Pharmacology* published by Wiley Periodicals LLC on behalf of the American Society for Clinical Pharmacology and Therapeutics. This is an open access article under the terms of the Creative Commons Attribution-NonCommercial-NoDerivs License, which permits use and distribution in any medium, provided the original work is properly cited, the use is non-commercial and no modifications or adaptations are made.